

Sloshing behavior of a magnetic fluid in a cylindrical container

T. Sawada, Y. Ohira, H. Houda

Abstract Sloshing of a magnetic fluid in a laterally vibrated cylindrical container subject to a non-uniform vertical magnetic field was examined. Internal velocity profiles were measured using ultrasound Doppler velocimetry. The effect of the magnetic field on the resonant frequency of the fluid–container system was examined and the results were compared with theoretical results. The second and third peaks of the power spectra of velocity shifted to lower frequencies as the magnetic field was increased. It was observed that these derived frequency peaks were connected with swirling in the cylindrical container.

1 Introduction

A magnetic fluid is a stable colloidal dispersion of rather small surfactant-coated magnetic particles in a liquid carrier. Magnetic fluids were developed in order to control the position of liquid fuel in a gravity-free state (Papell 1965). Fundamental studies have been made of some of the characteristics of magnetic fluids, such as strong magnetism and liquidity.

One interesting phenomenon of magnetic fluid motion is “sloshing”. Sloshing is the phenomenon observed when a liquid with a free surface is severely agitated in a liquid storage container. Zelazo and Melcher (1969) studied the dynamic behavior of a magnetic fluid in an oscillated container in order to investigate the influence of a tangential magnetic field on the resonance of surface waves. Dodge and Garza (1970) demonstrated a simulation of liquid sloshing in low gravity by using a magnetic fluid. Sudo et al. (1987) examined the interfacial instability of magnetic fluids in a rectangular container in the presence

of a magnetic field tangential to the interface and estimated stable configurations of the interface in various conditions. Sawada et al. (1993) and Matsuura et al. (1995) studied two-layer liquid sloshing of a magnetic fluid and a silicon oil in a rectangular container, and clarified the effects of magnetic field on the resonant frequency.

Sloshing of an ordinary liquid has also been of interest in a variety of engineering fields. However, studies of sloshing are not easy from a mathematical point of view, because obvious non-linearities occur, especially in the vicinity of the resonant frequency. When a liquid in an axisymmetrical container is subject to a harmonical lateral vibration, the free surface may rotate harmonically or non-harmonically around the central axis of the container. This phenomenon has been called “swirling”. The direction of the rotation is not fixed and may change irregularly, including coming to a stop.

This swirling motion of waves was investigated by Hutton (1963). Several studies of this interesting phenomenon in an axisymmetrical container have been attempted. Miles (1976) presented a formulation for weakly non-linear surface waves in a cylindrical container, and Miles (1984) derived evolution equations for horizontal resonant oscillation of a cylindrical container. He found that the problem is characterized by the following three parameters: damping, frequency offset, and depth/radius. Funakoshi and Inoue (1988) carried out experiments on surface waves using a cylindrical container oscillated horizontally with a period close to that associated with two known degenerate modes. They examined the irregular wave motion in detail from the standpoint of chaos in systems with only a few degrees of freedom.

In these studies, the most interesting aspect of sloshing has been the regular or irregular surface wave motions. It is necessary, however, to clarify the relationship between the surface waves and the inner fluid motion. Some numerical methods have been proposed to predict sloshing problems using complete Navier–Stokes equations (e.g., Partom 1987; Ramaswamy 1990). Ushijima (1998) proposed a numerical method to predict non-linear free surface oscillation in an arbitrary-shaped three-dimensional container subject to horizontal and vertical oscillations. He was able to predict non-linear sloshing motions in various conditions. Bauer and Eidel (1999) obtained natural damped frequencies and observed the response to translational excitation on a viscous liquid in a circular cylindrical container. They discussed the influence of the liquid–height ratio, surface tension parameter and Bond number on free surface oscillations in details. However,

Received: 9 May 2000 / Accepted: 29 May 2001
Published online: 29 November 2001

T. Sawada (✉), Y. Ohira¹, H. Houda
Department of Mechanical Engineering
Keio University 3-14-1 Hiyoshi, Kohoku-ku
Yokohama 223-8522, Japan
Fax: +81-45-5661495
e-mail: sawada@mech.keio.ac.jp

Present address: Pioneer Corporation,
Tokorozawa 359-8522, Japan

We should like to thank Dr. H. Kikura of Tokyo Institute of Technology for his collaboration in UVP measurements. This work was partially supported by a Grant-in-Aid for Scientific Research (B) of Japan Society for Promotion of Science.

there have been few experimental studies with respect to velocity field in sloshing because of the difficulty of measuring velocity profiles. The measurement of velocity profiles is even more difficult for magnetic fluid sloshing because magnetic fluids are opaque and optical methods such as laser Doppler anemometry or flow visualization techniques such as particle image velocimetry cannot be applied.

Takeda (1986) has developed an ultrasound velocity profile (UVP) measuring technique. It is a method of measuring a velocity profile along a beam line, that is, with respect to the velocity component along the ultrasound beam. This method can be applied to opaque fluids such as a liquid metal. For example, Takeda (1987) has studied its application to the flow of mercury. Experiments for velocity profile measurements of magnetic fluids have also been carried out. Kikura et al. (1999a, 1999b) examined Taylor vortex flow, sloshing flow and oscillating pipe flow of a magnetic fluid based on velocity distributions measured by the UVP method. Sawada et al. (1999a) measured the horizontal velocity profile of a magnetic fluid in a rectangular container which was laterally vibrated. The influence of magnetic fields on flow characteristics of a magnetic fluid have been clearly examined through these velocity profile measurements. The effectiveness of the UVP method for magnetic fluid flow problems has been recognized.

In the present paper, we measure the velocity profile of a magnetic fluid in a cylindrical container. When a magnetic field is applied to a magnetic fluid, each of sloshing, free surface wave motion, swirling motion and velocity profile change according to the magnetic field intensity. In order to clarify the effects of a magnetic field on flow behavior, experiments are performed for several conditions.

2

Facilities and experimental conditions

The experimental apparatus is shown schematically in Fig. 1. Specific dimensions in relation to the cylindrical container are indicated in Fig. 2. The cylindrical container is made of Plexiglas, and its inner diameter and height are 94 mm and 300 mm, respectively. Rotation of a motor is changed to horizontal motion by an adjustable crank mechanism. The adjustable crank is mounted on the output shaft of the motor and connects to a vibrating table which holds the cylindrical container. The rotational frequency of the motor is continuously controlled by an inverter. The vibrating table is oscillated sinusoidally, and has a range of oscillation from 0.42 Hz to 4.17 Hz. The amplitude of the oscillation is $X_0 = 1.5$ mm for all experiments. The frequency and amplitude of oscillation is measured by a laser displacement sensor.

A magnetic field is applied by a cylindrical permanent magnet whose diameter is 110 mm. We used several different permanent magnets in order to change the magnetic field intensity. The distributions of the magnetic field induction B along the normal central line for each of the permanent magnets are shown in Fig. 3. Here B_0 is the surface magnetic field induction at the center of the permanent magnet and h_m is the distance from the permanent magnet. These distributions of magnetic field induction are used for the theoretical calculations.

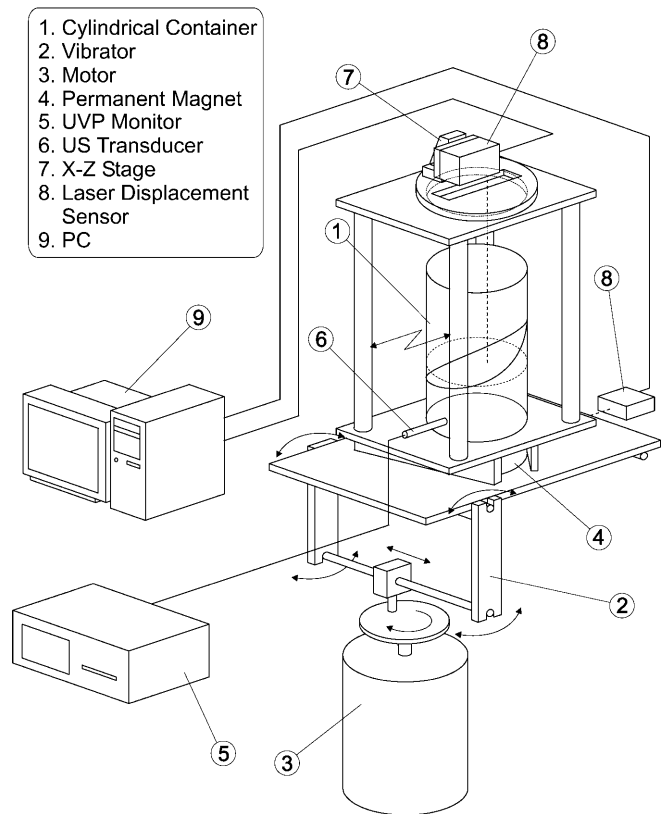


Fig. 1. Experimental apparatus

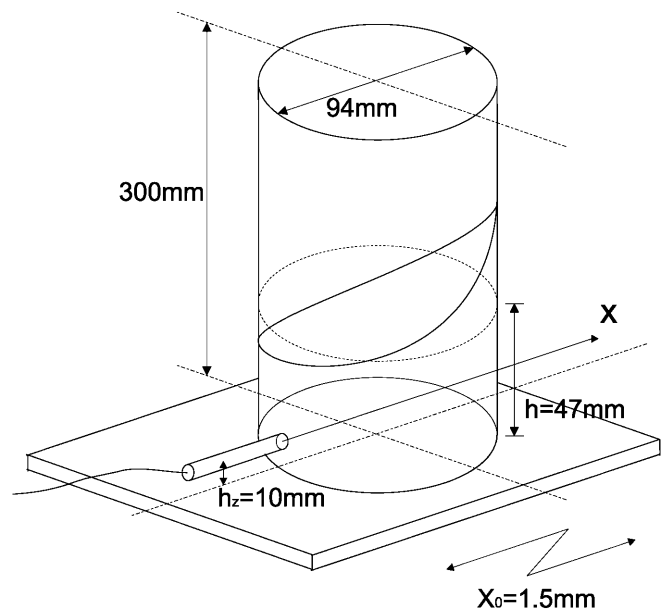


Fig. 2. Cylindrical container

The magnetic fluid is a water-based 27% weight concentration of fine magnetite particles, Fe_3O_4 . Its kinematic viscosity, density and sound velocity are $\nu = 2.8 \times 10^{-6}$ m^2/s , $\rho = 1.21 \times 10^3$ kg/m^3 and $c = 1,420$ m/s at 25°C , respectively. The fluid depth is $h = 47$ mm. Though magnetic fluids have many magnetic particles, they are too small to reflect ultrasonic waves. We add, therefore, porous SiO_2 particles with a mean diameter of $0.9 \mu\text{m}$

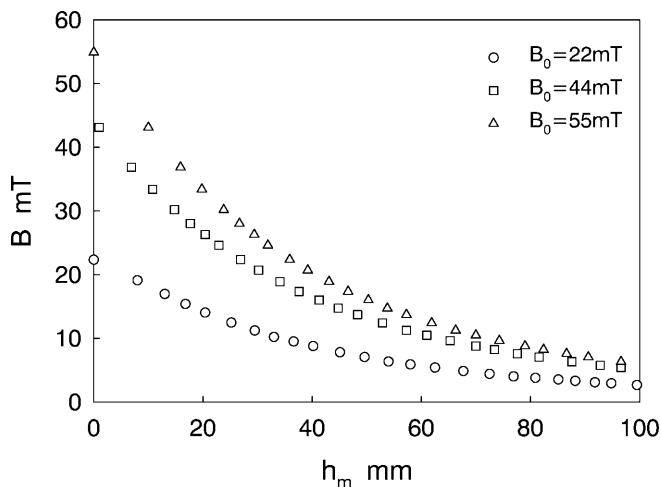


Fig. 3. Distribution of magnetic field induction along the normal central line of the permanent magnet

as reflectors. The mean diameter of the added particles is still less than the wavelength of the ultrasound but the power of the reflected echo is sufficient to obtain a good signal-to-noise ratio for computing velocity because of the clustering and chaining of the magnetic and reflector particles (Sawada et al. 1999b).

An ultrasonic (US) transducer is fixed on the side wall of the container. Its position is fixed at $h_z = 10$ mm height. The nominal diameter of the US transducer is 5 mm, and the measuring volume has a thin-disc shape, ϕ 5 mm \times 0.71 mm. The UVP monitor is a Model X-3 manufactured by Met-Flow SA. The basic frequency is 4 MHz and the pulse repetition frequency is 2,916 Hz. There are 128 measurement points along the measurement axis (x -axis). The free surface elevation is measured by a second laser displacement sensor.

3 Linearized approach

Our analytical model uses the cylindrical coordinates r , θ , and z , as shown in Fig. 4, where z is upward vertically measured from the mean position of the free surface. R is the radius of the cylindrical container, h is the fluid depth, and X_0 and ω are the amplitude and angular forcing frequency of the oscillation of the vibrating table, respectively.

With the assumptions of irrotational flow and an incompressible fluid, a velocity potential ϕ exists which should satisfy the continuity equation:

$$\frac{\partial^2 \phi}{\partial r^2} + \frac{1}{r} \frac{\partial \phi}{\partial r} + \frac{1}{r^2} \frac{\partial^2 \phi}{\partial \theta^2} + \frac{\partial^2 \phi}{\partial z^2} = 0 \quad (1)$$

The unsteady Bernoulli equation for a magnetic fluid (e.g., Rosensweig 1985) is given by

$$\rho \frac{\partial \phi}{\partial t} + \frac{1}{2} \rho |\nabla \phi|^2 + p + \rho g z - \mu_0 \int_0^H M dH = \rho X_0 \omega^2 r \sin \omega t \quad (2)$$

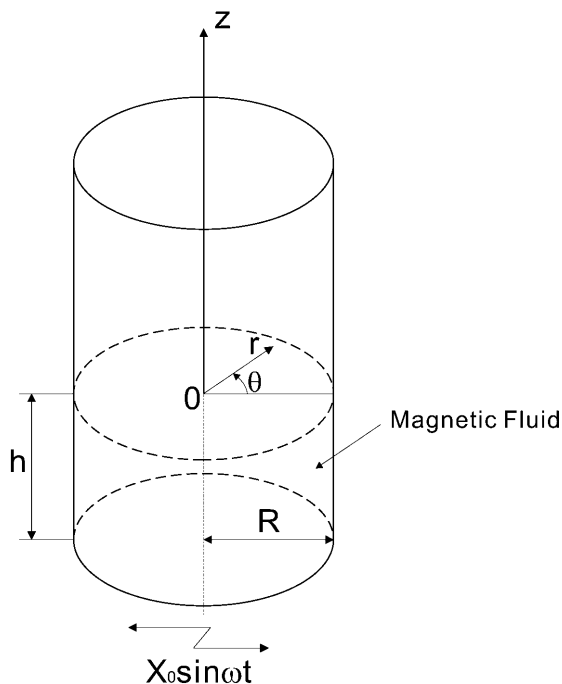


Fig. 4. Analytical model

where p , g , μ_0 , M and H are pressure, gravitational acceleration, magnetic permeability of vacuum, magnetization, and magnetic field, respectively. When the magnetization and magnetic field are assumed to be parallel, the last integration term on the left-hand side of Eq. (2) can be written as

$$\int_0^H M dH = \frac{1}{2} \chi H^2 \quad (3)$$

where χ is the susceptibility of the magnetic fluid. The magnetic field $H(z)$ is approximated by

$$H(z) = H_0 e^{-\alpha(z+h)} \quad (4)$$

where H_0 is the magnetic field intensity at the bottom of the container ($z = -h$) and α is a constant which is determined by measurement of the magnetic field as shown in Fig. 3. For infinitesimally small waves, it is assumed that $|\nabla \phi|^2$ is negligible. Since pressure is constant on the free surface, evaluating Eq. (2) on $z = \eta(r, \theta, t)$ by expanding the value of the condition at $z = 0$ by the truncated Taylor series yields the kinematic and dynamic free surface conditions (e.g., Dean and Dalrymple 1984):

$$\frac{\partial \eta}{\partial t} = \left(\frac{\partial \phi}{\partial z} \right)_{z=0} \quad (5)$$

$$\left(\frac{\partial^2 \phi}{\partial t^2} + g^* \frac{\partial \phi}{\partial z} \right)_{z=0} = X_0 \omega^3 r \cos \omega t \quad (6)$$

where g^* is the effective gravity due to the magnetic force and is given by

$$g^* = g + \frac{\alpha \mu_0 \chi H_0^2 e^{-2\alpha h}}{\rho} \quad (7)$$

Boundary conditions on the bottom and side walls are given by

$$\left(\frac{\partial\phi}{\partial z}\right)_{z=-h} = 0 \quad (8)$$

$$\left(\frac{\partial\phi}{\partial r}\right)_{r=R} = 0 \quad (9)$$

Equation (1) is solved by using Eqs. (5), (6), (8) and (9) to provide:

$$\phi = \sum_{m=1}^{\infty} \sum_{n=1}^{\infty} \left\{ \begin{aligned} & A_{mn} J_m(k_{mn} r) \cos(m\theta + \delta_{mn}) \cosh k_{mn}(z+h) \cos(\omega_{mn} t + \varepsilon_{mn}) \\ & + \frac{\omega_{mn}^2 \omega^3}{\omega_0^2 - \omega^2} \frac{r X_0 \cosh k_{mn}(z+h) \cos \omega t}{g^* k_{mn} \sin h k_{mn} h} \end{aligned} \right\} \quad (10)$$

where J_m is the Bessel function of the first kind, of order m , and A_{mn} , δ_{mn} and ε_{mn} are arbitrary constants. The value of k_{mn} is chosen so that $k_{mn}R$ is the zero of J_m . Also, here ω_{mn} is the characteristic angular frequency given by

$$\omega_{mn} = \sqrt{g^* k_{mn} \tanh(k_{mn} h)} \quad (11)$$

4

Results and discussion

Figure 5 shows the frequency response of the free surface of the magnetic fluid as the forcing frequency varies. The surface magnetic field induction at the center of the permanent magnet is indicated by B_0 , η is the maximum free surface elevation at the inner wall, f is the forcing frequency, and f_0 is the first resonant frequency for $B_0 = 0$ mT calculated by Eq. (11). Figures 6 and 7 are illustrations provided to aid the understanding of the sloshing and swirling motion.

For $B_0 = 0$ mT, sloshing behavior is explained as follows. In region A, the free surface vibrates in the direction of the forced oscillation. As the forcing frequency increases, the surface elevation also increases until the free surface shakes more intensely when nearing the resonant frequency (border between A and B). At the resonant frequency, the free surface forms a collapsed wave, and

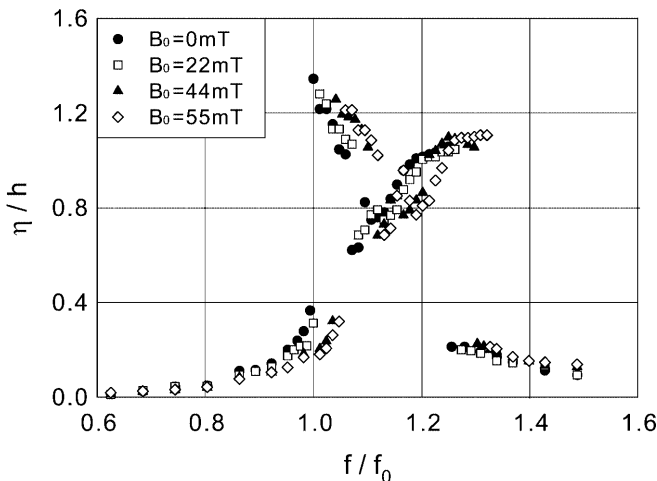


Fig. 5. Frequency response of the free surface

after the resonant frequency (in region B), rotation around the center axis of the container occurs. The direction of the rotation is not fixed, and changes irregularly. This phenomenon is named “unstable swirling” (see Figs. 6 and 7). As the forcing frequency increases in region B, the surface elevation decreases with unstable swirling. On the border between B and C, the unstable swirling changes to swirling in which the direction is fixed. This phenomenon has been named “stable swirling” (see Figs. 6 and 7). In region C, the stable swirling is in a direction that depends on the

direction of the unstable swirling at the border between B and C. As the forcing frequency increases further, the surface elevation increases. The surface elevation reaches a local maximum again on the border between C and D and rapidly decreases just after the border. In region D, the free surface vibrates in a similar manner to region A. When a magnetic field is applied, each of regions A, B, C and D move to higher frequencies according to the intensity of the magnetic field.

In Figs. 8 and 9, the experimental results are compared with the linear theoretical results for $B_0 = 0$ mT and 55 mT. The experimental resonant frequencies agree with the theoretical results, and the shift of the resonant frequency due to the magnetic field is verified. This increase in the resonant frequency with a magnetic field is caused by an increase in the effective gravity expressed by Eq. (7). Note, however, for large free surface elevations, there are some differences between experimental and theoretical results because of the use of linearized theory.

UVP measurements were made for the stable swirling region (region C). We calculated power spectra from the

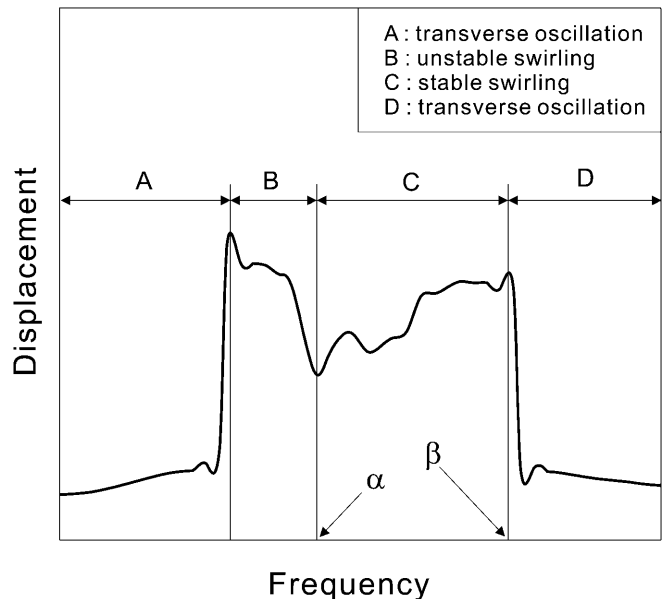


Fig. 6. Illustration of frequency response of the free surface

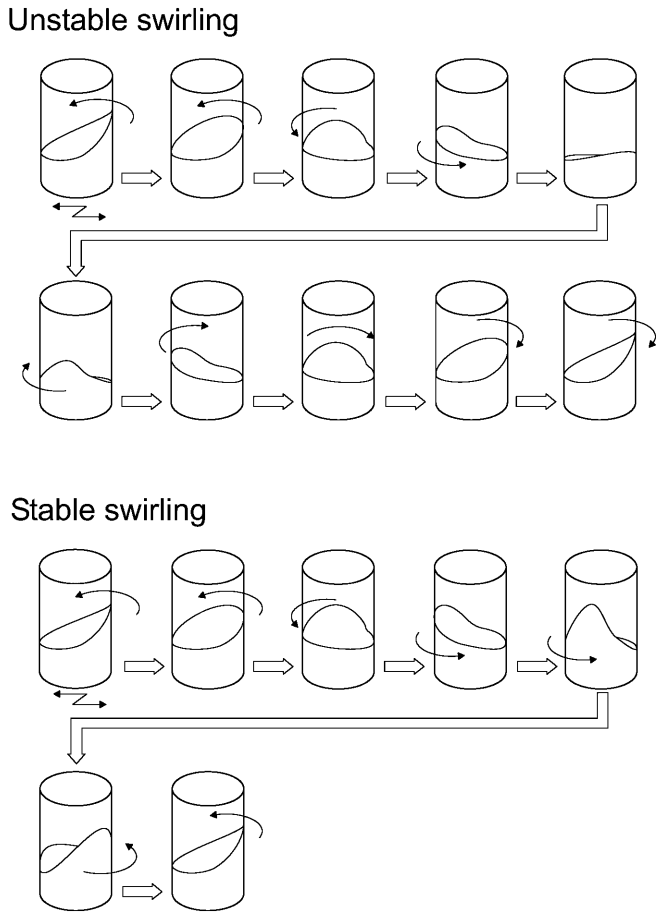


Fig. 7. Unstable and stable swirling

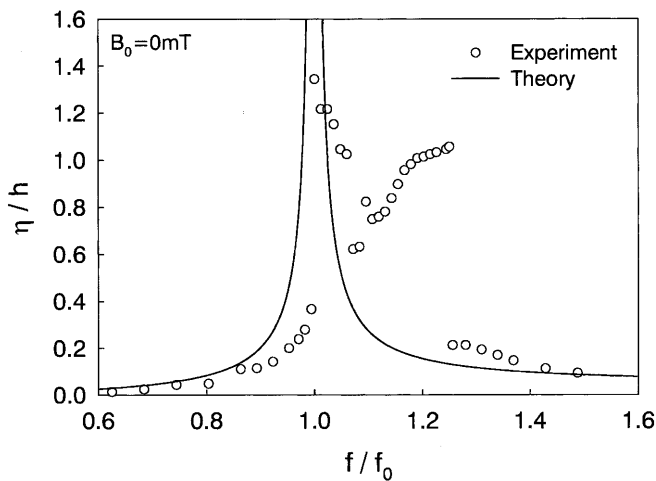


Fig. 8. Comparison of theoretical and experimental results for frequency response of surface elevation for $B_0 = 0$ mT

measured velocity data by using a fast Fourier transform in the time domain. Figure 10 shows the power for the α -frequency averaged over a region of $0.474 \leq r/R \leq 0.534$ at $h_z = 10$ mm. The α -frequency is the frequency where unstable swirling changes to stable swirling indicated as point α in Fig. 6. The horizontal averaging area corresponds to $44.6 \text{ mm} \leq x \leq 50.2 \text{ mm}$. Figure 11 shows the

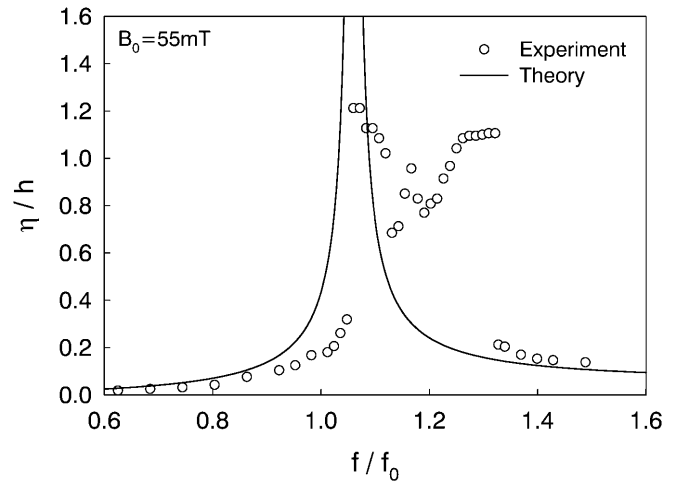


Fig. 9. Comparison of theoretical and experimental results for frequency response of surface elevation $B_0 = 55$ mT

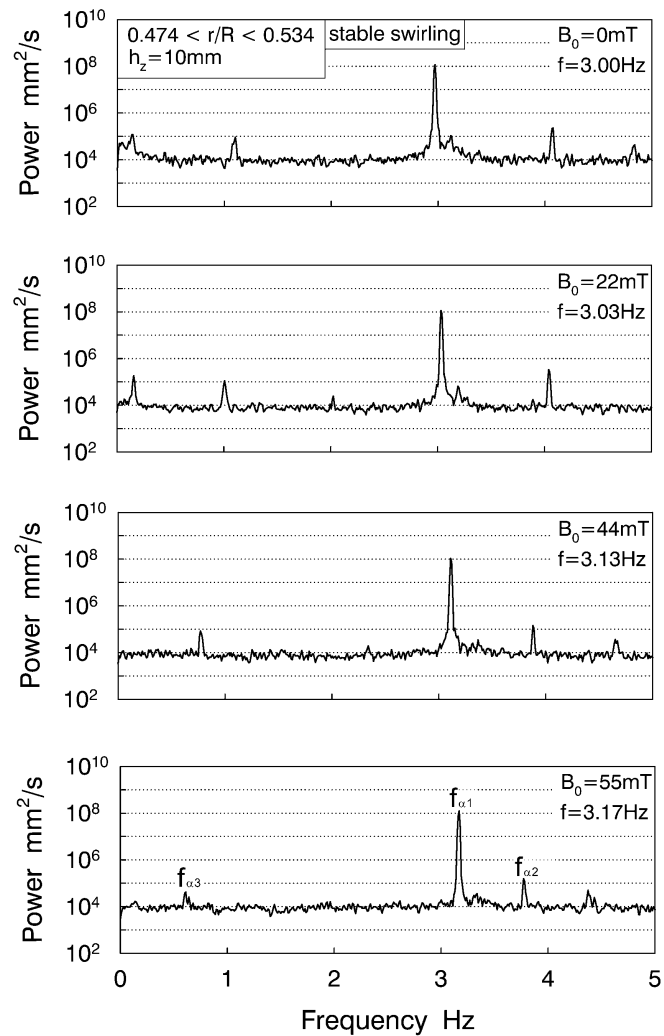


Fig. 10. Averaged power spectra of velocity oscillations for α -frequency

power for the β -frequency. The β -frequency is the frequency where the stable swirling of the fluid changes to simple oscillation, as indicated by point β in Fig. 6.

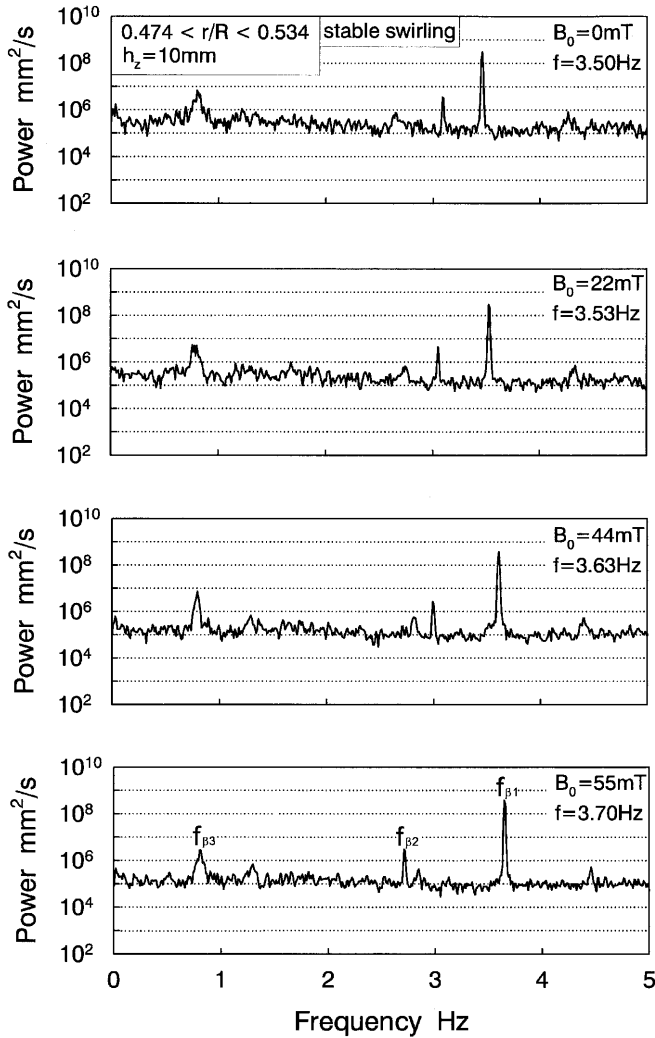


Fig. 11. Averaged power spectra of velocity oscillations for β -frequency

The most dominant peaks, f_{x1} and $f_{\beta1}$, for each applied magnetic field correspond to the forcing frequency. For each applied magnetic field, there are also a few derived peaks. As the magnetic field is increased, the second and third dominant peaks except $f_{\beta3}$ shift to lower frequencies. The frequency f_{x3} is approximately equal to the frequency difference $f_{x2} - f_{x1}$. It may be explained as a consequence of the non-linear nature of the oscillations. However, here the direction of forced oscillation and measuring line of the velocity profile are the same, and we believe that it is necessary to carry out more velocity measurements along other directions in order to more fully understand the behavior of the derived peaks.

When a magnetic field is applied, the disturbance of the fluid is suppressed (as seen by comparing Figs. 8 and 9). In our previous study of a magnetic fluid sloshing in a rectangular container (Sawada et al. 1999a), a decrease in the free surface elevation and the height of peak spectra of horizontal velocity were observed. However, in a cylindrical container, the height of each peak of velocity oscillations hardly changes with magnetic field intensity. It is thus believed that these derived peaks have some relevance to swirling.

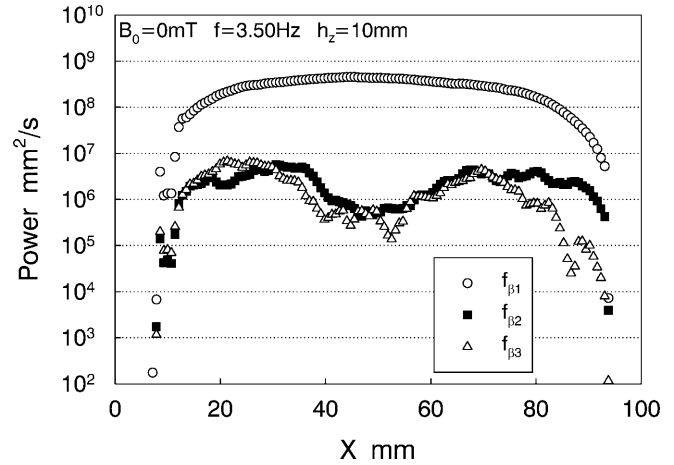


Fig. 12. Spatial distribution of the power spectra of velocity oscillations for β -frequency at $B_0 = 0$ mT

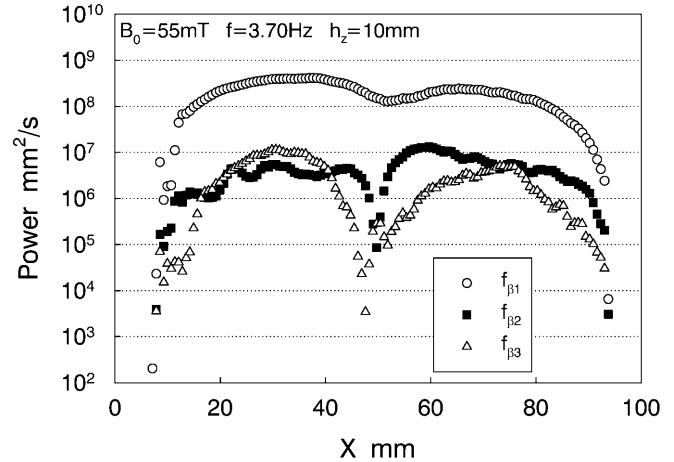


Fig. 13. Spatial distribution of the power spectra of velocity oscillations for β -frequency at $B_0 = 55$ mT

In Figs. 12 and 13, the spatial spectra for the β -frequencies ($f_{\beta1}$, $f_{\beta2}$, $f_{\beta3}$) are shown for the cases $B_0 = 0$ mT and $B_0 = 55$ mT, respectively. Here x is the distance from the inner wall, that is, $x = 0$ corresponds to $r = R$ and $\theta = \pi$ (see Fig. 2). Since the velocity component is measured in the r -direction, the power decreases abruptly near the wall. An indentation or depression is observed in the distributions for $f_{\beta2}$ and $f_{\beta3}$ near the center of the cylindrical container. This indentation seems to be caused by the swirling phenomenon. Further, this indentation is not observed for the $f_{\beta1}$ distribution in Fig. 12 but a small indentation is observed for $B_0 = 55$ mT in Fig. 13. We believe this is because lateral oscillation of the magnetic fluid is suppressed by the magnetic field.

5 Concluding remarks

Lateral sloshing of a magnetic fluid in a cylindrical container in a vertically applied non-uniform magnetic field was studied. The effects of the magnetic field on the free surface elevation were examined. We also compared the experimental shift of the first resonant frequency with linearized theoretical

results obtained by assuming a potential flow and infinitesimally small waves.

Since a magnetic fluid is opaque, it has been very difficult to obtain velocity profiles using conventional measuring methods. We have successfully applied the UVP measurement technique to magnetic fluid sloshing to obtain both time dependent velocity profiles and spatial velocity profiles along horizontal lines. We found that the amplitude of the velocity decreases with an increase in the magnetic force. Also, the power spectra were calculated from the velocity data. The most dominant peak of the power spectrum moves to a higher frequency as the magnetic field intensity increases. However, derived second and third peaks shift to a lower frequency. We believe that these derived peaks will be the key to a detailed understanding of swirling phenomena. However, further study is required before the mechanism can be clarified. From the observed spatial distribution of the power spectra, it seems that the swirling motion of a fluid is characterized by the derived peak frequencies. In order to clarify the swirling mechanism using velocity profiles, we believe it will be useful to obtain spatial velocity distributions of the whole area simultaneously by using several US transducers (Takeda and Kikura 1998).

Another potential problem in the present study may be the use of a permanent magnet that is not significantly larger than the test cell to apply the magnetic field. The magnetic field gradient is not exactly normal to the free surface, and thus the direction of the magnetic body force is oblique with respect to the central line of the cylindrical container. Moreover, the intensity and direction of the magnetic body force changed with the magnetic field intensity, which may have a strong effect on the swirling motions and the shift of the derived power spectra.

References

- Bauer HF; Eidel W** (1999) Free oscillations and response of a viscous liquid in a rigid circular cylindrical tank. *Aerosp Sci Technol* 3: 495–512
- Dean RG; Dalrymple RA** (1984) *Water wave mechanics for engineers and scientists*, Chap. 3. Prentice Hall, Englewood Cliffs, NJ
- Dodge FT; Garza LR** (1970) Magnetic fluid simulation of liquid sloshing in low gravity. NASA Tech Rep 9: 1–29
- Funakoshi M; Inoue S** (1988) Surface waves due to resonant horizontal oscillation. *J Fluid Mech* 192: 219–247
- Hutton RE** (1963) An investigation of resonant, nonlinear, non-planar free surface oscillations of a fluid. NASA Tech Note D-1870
- Kikura H; Takeda Y; Durst F** (1999a) Velocity profile measurement of the Taylor vortex flow of a magnetic fluid using the ultrasonic Doppler method. *Exp Fluids* 26: 208–214
- Kikura H; Takeda Y; Sawada T** (1999b) Velocity profile measurements of magnetic fluid flow using ultrasonic Doppler method. *J Magn Magn Mater* 201: 276–280
- Matsuura F; Matsubara Y; Sawada T; Tanahashi T** (1995) Surface behaviors of two-layers liquid sloshing under non-uniform magnetic field. In: Hahn SY (ed) *Advanced computational and design techniques in applied electronic systems*. Elsevier Science, Amsterdam, pp 517–520
- Miles JW** (1976) Nonlinear surface waves in closed basins. *J Fluid Mech* 75: 419–448
- Miles JW** (1984) Resonantly forced surface waves in a circular cylinder. *J Fluid Mech* 149: 15–31
- Papell SS** (1965) Low viscosity magnetic fluid obtained by the colloidal suspension of magnetic particles. US Patent 3215572
- Partom LS** (1987) Application of the VOF method to the sloshing of a fluid in a partially filled cylindrical container. *Int J Numer Meth Fluids* 7: 535–550
- Ramaswamy B** (1990) Numerical simulation of unsteady viscous free surface flow. *J Comput Phys* 90: 396–430
- Rosensweig RE** (1985) *Ferrohydrodynamics*. Cambridge University Press, Cambridge
- Sawada T; Kikura H; Shibata S; Tanahashi T** (1993) Lateral sloshing of a magnetic fluid in a container. *J Magn Magn Mater* 122: 424–427
- Sawada T; Kikura H; Tanahashi T** (1999a) Kinematic characteristics of magnetic fluid sloshing in a rectangular container subject to non-uniform magnetic fields. *Exp Fluids* 26: 215–221
- Sawada T; Kikura H; Yamanaka G; Matsuzaki M; Nakatani I; Aritomi M** (1999b) Visualization of clustering on non-magnetic and ferromagnetic particles in magnetic fluids. *Proc SPIE* 3783: 389–396
- Sudo S; Hashimoto H; Katagiri K** (1987) Interfacial instability of magnetic fluids in a rectangular container. *JSME Int J* 30: 1086–1092
- Takeda Y** (1986) Velocity profile measurement by ultrasound Doppler shift method. *Int J Heat Fluid Flow* 7: 313–318
- Takeda Y** (1987) Measurement of velocity profile of mercury flow by ultrasound Doppler shift method. *Nucl Technol* 79: 120–124
- Takeda Y; Kikura H** (1998) Measurement of mercury flow by ultrasonic Doppler method. *Proceedings of the 1998 ASME Fluid Engineering Division Summer Meeting*. FEDSM98-5074: CD-ROM
- Ushijima S** (1998) Three-dimensional arbitrary Lagrangian-Eulerian numerical prediction method for non-linear free surface oscillation. *Int J Numer Meth Fluids* 26: 605–623
- Zelazo RE; Melcher JR** (1969) Dynamics and stability of ferrofluids surface interaction. *J Fluid Mech* 39: 1–24